S1

A

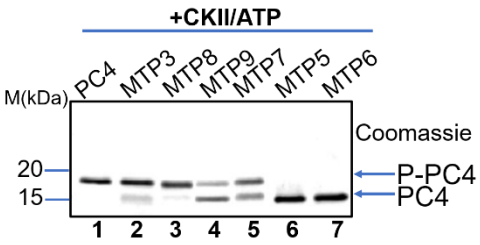

B

Name	Residues Mutated	Phosphorylation Ability
PC4		++++
MTP3	17	++
MTP8	13,17	+++
MTP9	15, 17	-/+
MTP7	13,15	++/-
MTP5	13,15,17,19	-
MTP6	13, 15, 17	-

C

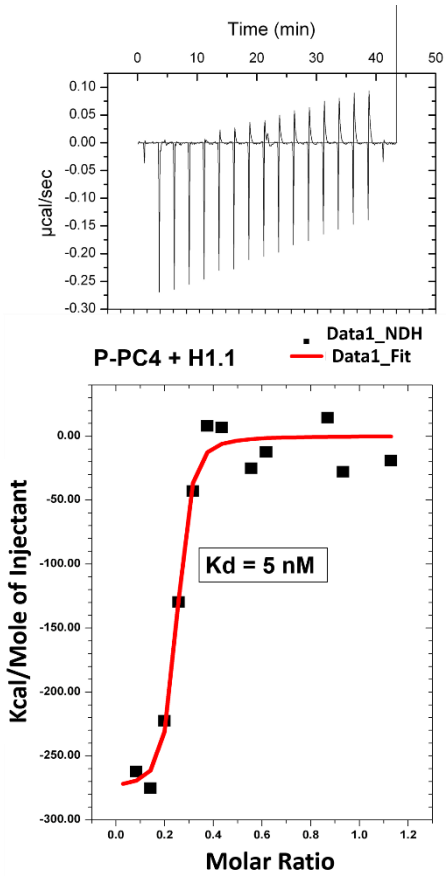

D

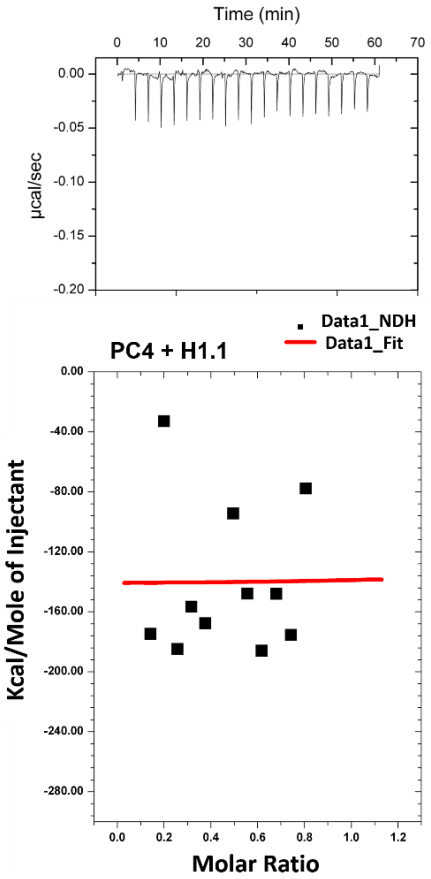

FigureS1. Casein Kinase II mediated phosphorylation of PC4 is critical for its interaction with linker histone H1. (A) *In vitro* kinase assay performed using 600ng of wild type and different phospho-defective mutants using [Υ^{32}P] ATP and commercially available casein kinase II (CKII) enzyme. (B) Table illustrating the extent of phosphorylation ability of different serine mutants of PC4. (C) Isothermal calorimetric titration of P-PC4 (Phosphorylated PC4 which has been re-purified after kinase assay) with linker H1.1 and (D) PC4-H1.1 were carried out to determine the enthalpy change and stoichiometry of interaction.

S2

A

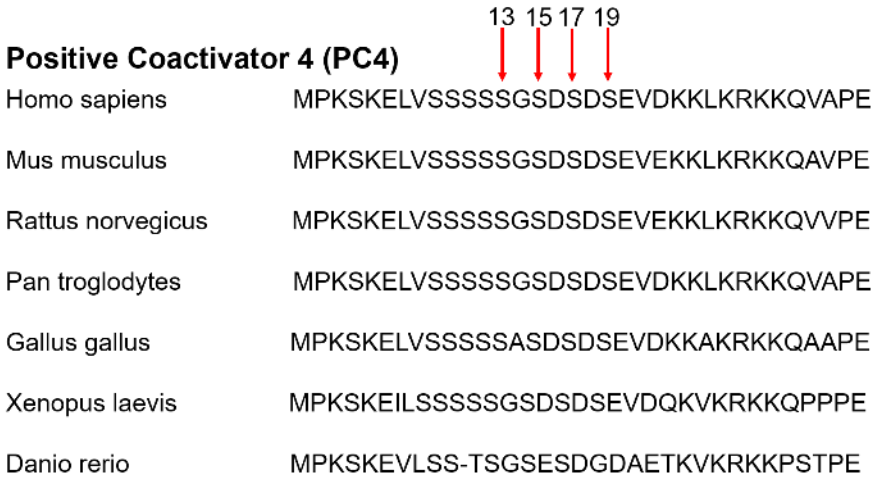
13 15 17 19
Positive Coactivator 4 (PC4)
Homo sapiens MPKSKELVSSSSSGSDSDSEVDKKLKRKKQVAPE
Mus musculus MPKSKELVSSSSSGSDSDSEVEKKLKRKKQAVPE
Rattus norvegicus MPKSKELVSSSSSGSDSDSEVEKKLKRKKQVVPE
Pan troglodytes MPKSKELVSSSSSGSDSDSEVDKKLKRKKQVAPE
Gallus gallus MPKSKELVSSSSSASDSDSEVDKKAKRKKQAAPE
Xenopus laevis MPKSKEILSSSSSGSDSDSEVDQKVKRKKQPPPE
Danio rerio MPKSKEVLSS-TSGSESDGDAETKVKRKKPSTPE

B

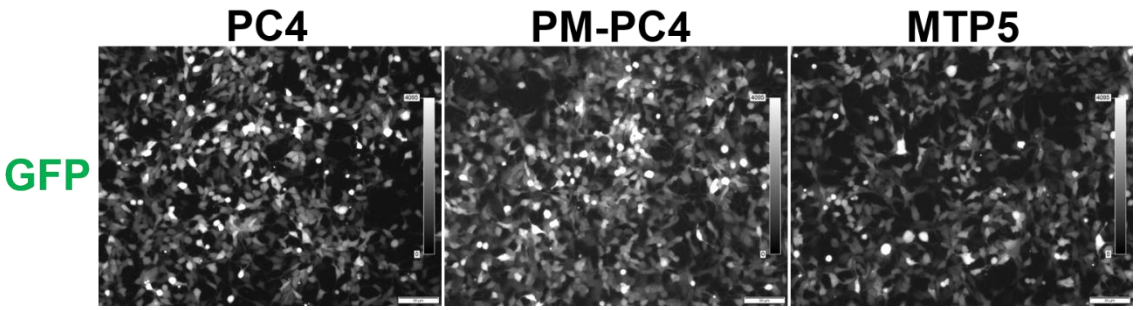
PC4
PM-PC4
MTP5
GFP

C

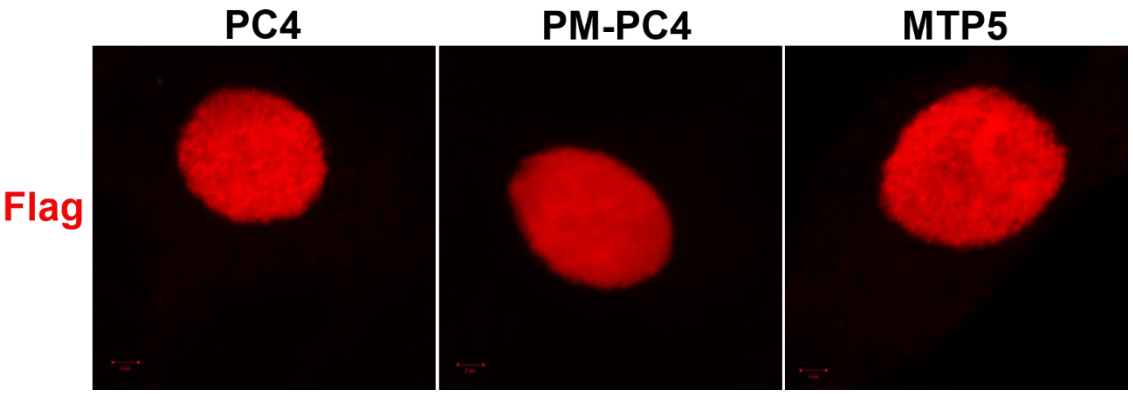
PC4
PM-PC4
MTP5
Flag

D

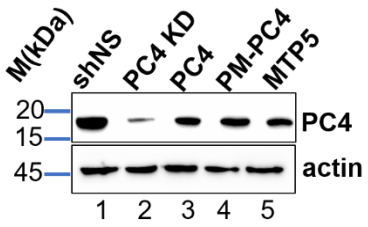
M(kDa)
shNS
PC4 KD
PC4
PM-PC4
MTP5
20
15
45
PC4
actin
1 2 3 4 5

FigureS2. Phosphomimic PC4 (PM-PC4) interacts with linker histone H1. (A) Alignment of PC4 (*Homo sapiens*) surrounding the four serine residues 13,15,17 and 19 in different species. (B) HEK 293 cells transfected with PC4, PM-PC4 and MTP5 was analysed for GFP by fluorescent microscopy to validate the cellular localization of the PC4 constructs in pGIPZ vector backbone. (C) HEK 293 cells transfected with PC4, PM-PC4 and MTP5 in PC4 knockdown background was analysed for their subcellular localisation by fluorescent microscopy using anti-flag antibody. (D) Studying PC4 expression by western blotting in Flag tagged PC4, PM-PC4 and MTP5 expressing PC4 knockdown cells along with PC4 knockdown (PC4 KD) and vector control cells (shNS).

S3

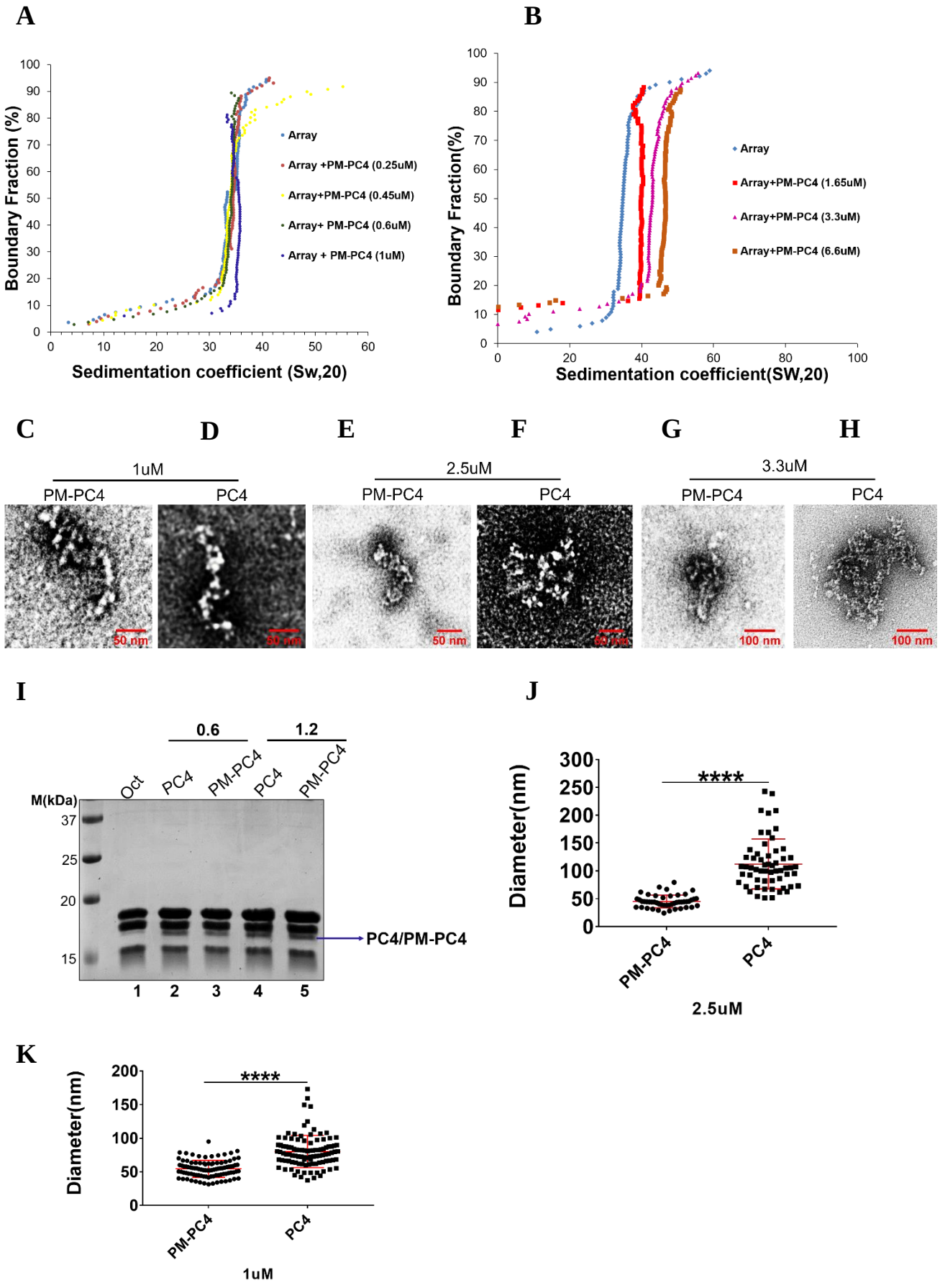
A
Boundary Fraction (%)
Sedimentation coefficient (Sw,20)
Array
Array +PM-PC4 (0.25uM)
Array+PM-PC4 (0.45uM)
Array+ PM-PC4 (0.6uM)
Array + PM-PC4 (1uM)
B
Boundary Fraction(%)
Sedimentation coefficient(SW,20)
Array
Array+PM-PC4 (1.65uM)
Array+PM-PC4 (3.3uM)
Array+PM-PC4 (6.6uM)
C D E F G H
1uM
2.5uM
3.3uM
PM-PC4
PC4
50 nm
100 nm
I
0.6
1.2
Oct
PC4
PM-PC4
PC4
PM-PC4
M(kDa)
37
25
20
15
PC4/PM-PC4
1 2 3 4 5
J
Diameter(nm)
****
PM-PC4
PC4
2.5uM
K
Diameter(nm)
****
PM-PC4
PC4
1uM

FigureS3: Phosphomimic PC4 promotes condensation of an *in vitro* reconstituted nucleosomal array. (A-B) Sedimentation velocity analysis by analytical ultracentrifugation upon titrating a wide range of PM-PC4 (phosphomimic PC4) bound nucleosome array. (C-H) EM images of nucleosome array upon compaction with increasing concentration of PM-PC4 (phosphomimic PC4) (C,E and G) and PC4 (wild type unmodified recombinant) (D, F and H) respectively. (I) SDS-PAGE analysis of the ratio of PC4 and PM-PC4 input to octamers used in (Fig.3B). (J) Distribution of diameters (in nm) of PM-PC4 and PC4 bound compacted array particles. No. of particles measured = 60. Data represent the means ± SD. The S50%(S) were statistically analysed by Student's unpaired *t*-test (*p<0.05,**p<0.01,***p<0.001,ns-non-significant). (K) Distribution of diameters (in nm) of PM-PC4 and PC4 bound compacted array particles . No. of particles measured = 102. Data represent the means ± SD. The S50%(S) were statistically analysed by Student's unpaired *t*-test (*p<0.05,**p<0.01,***p<0.001,ns-non-significant).

S4

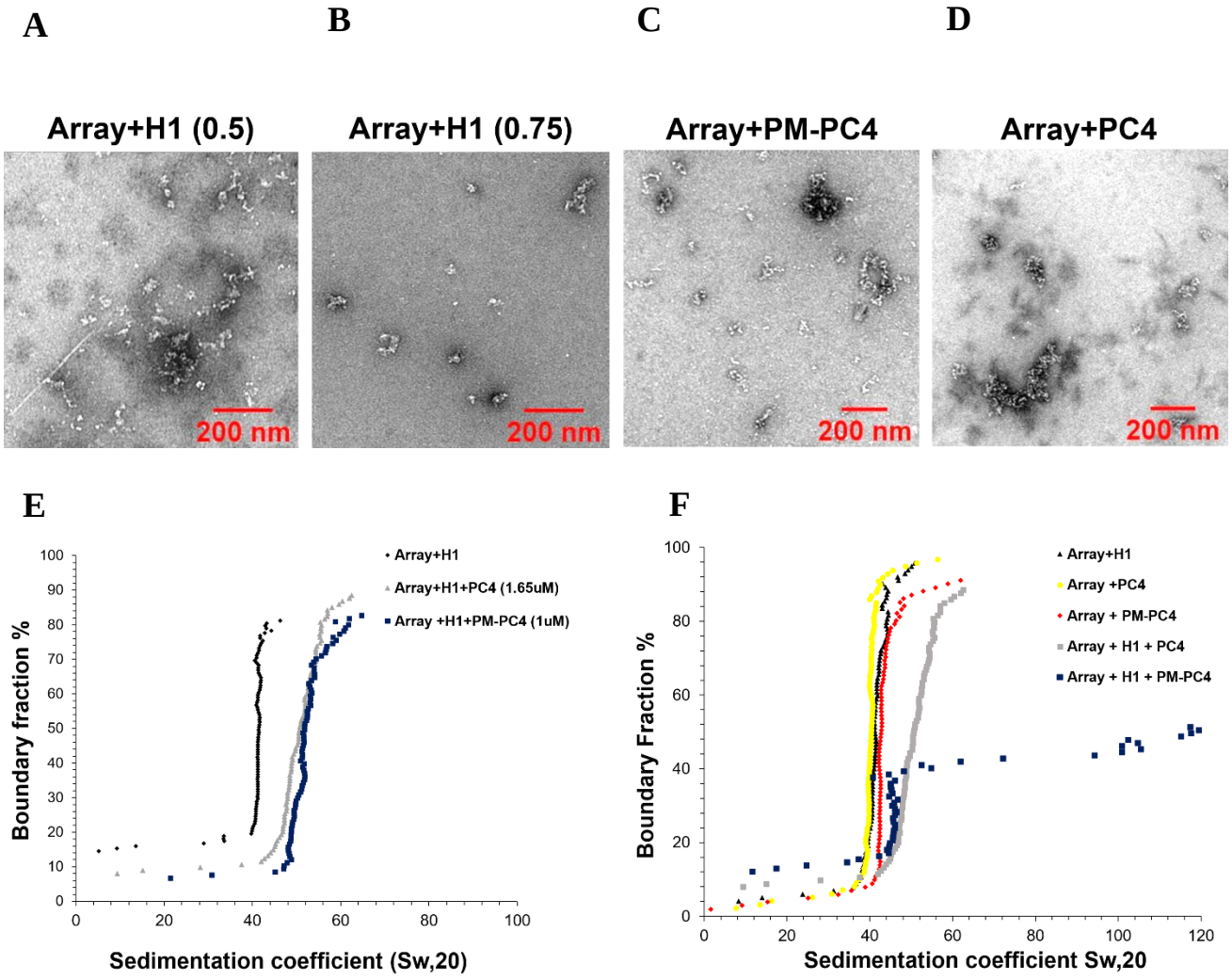
A
B
C
D
Array+H1 (0.5)
Array+H1 (0.75)
Array+PM-PC4
Array+PC4
200 nm
200 nm
200 nm
200 nm
E
Boundary fraction %
Sedimentation coefficient (Sw,20)
Array+H1
Array+H1+PC4 (1.65uM)
Array +H1+PM-PC4 (1uM)
F
Boundary Fraction %
Sedimentation coefficient Sw,20
Array+H1
Array +PC4
Array + PM-PC4
Array + H1 + PC4
Array + H1 + PM-PC4
G
M(kDa)
Oct
H1
PC4
PM-PC4
H1 +PC4
H1+ PM-PC4
37
25
20
15
H1
PC4/PM-PC4
1
2
3
4
5
6

Figure S4: Phosphorylation enhances PC4 mediated condensation of H1 bound array forming higher order structures. (A-B) EM images of H1 bound array in the ratio of H1: NCP of 0.5 and 0.75 respectively. (C-D) 1uM of PC4 (wild type unmodified recombinant) and PM-PC4 (phosphomimic PC4) containing array respectively. (E) Sedimentation velocity analysis by analytical ultracentrifugation of H1 containing chromatin (H1:NCP is 0.5) with PM-PC4 (1uM) and PC4 (1.65uM). H1 containing nucleosome array was used as a control. (F) Sedimentation velocity analysis of H1 containing nucleosome (H1:NCP is 0.5) incubated with 1.65uM of PM-PC4 (phosphomimic PC4) and PC4 (wild type unmodified recombinant) shows aggregation of the H1-bound array in the presence of PM-PC4. A nucleosome array without any protein is used as a control. (G) SDS-PAGE analysis of the ratio of H1, PC4 and PM-PC4 input to octamers used in (Fig.4A).

S5

Lane 1

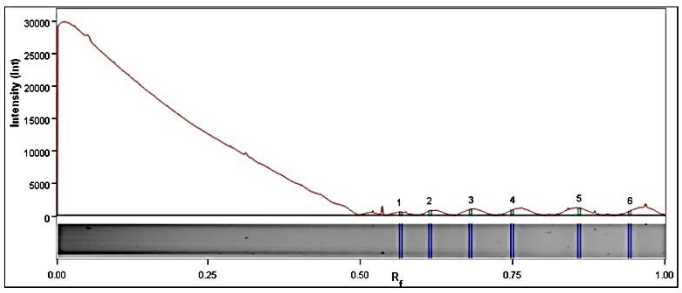

Lane 2

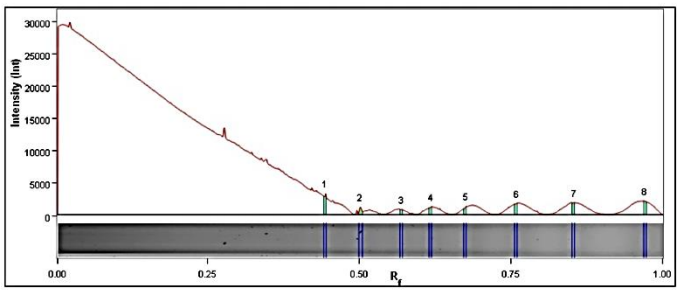

Lane 3

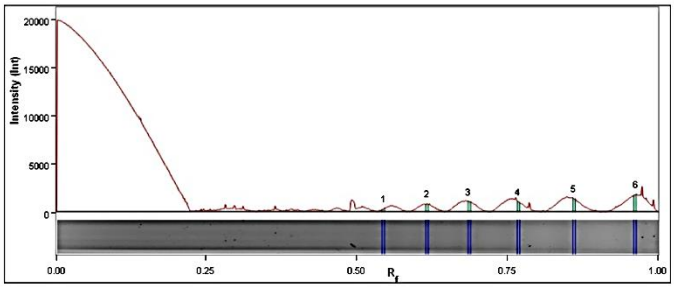

Lane 4

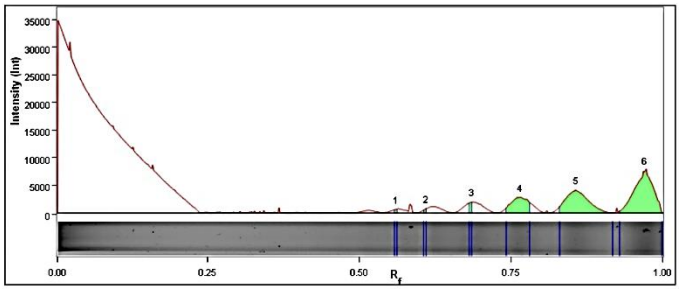

Lane 5

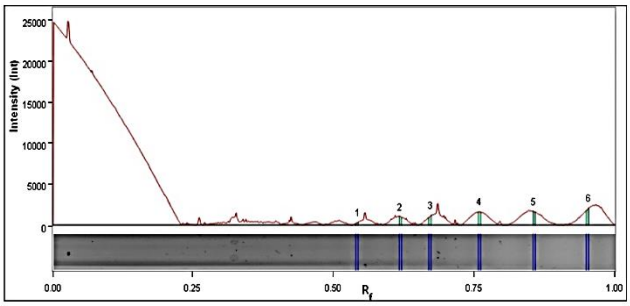

Lane 6

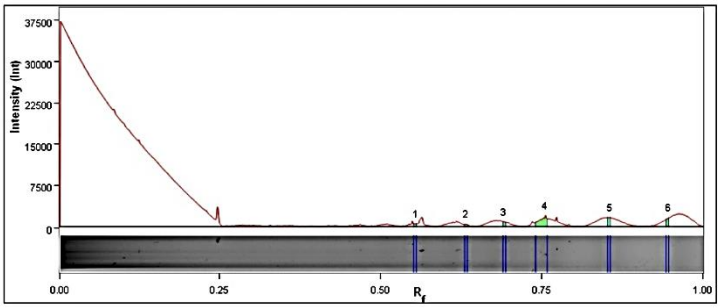

Lane 7

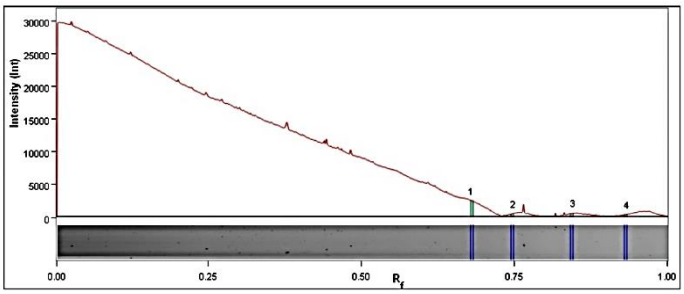

Lane 8

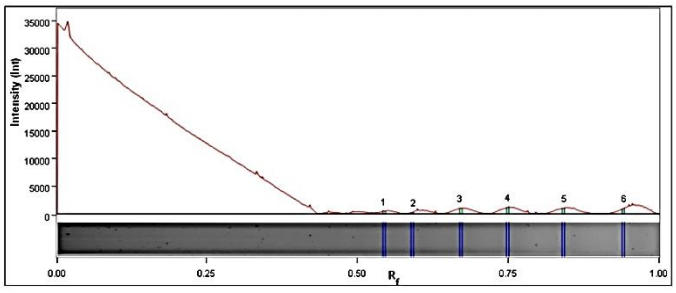

Lane 9

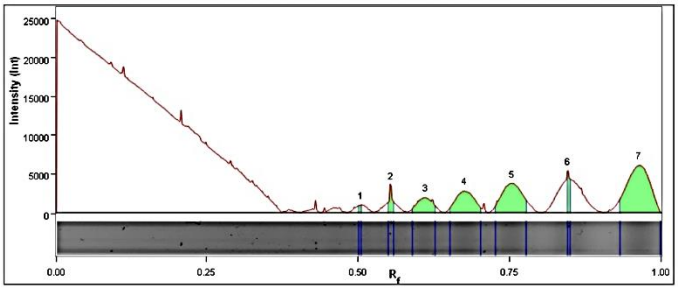

Lane 10

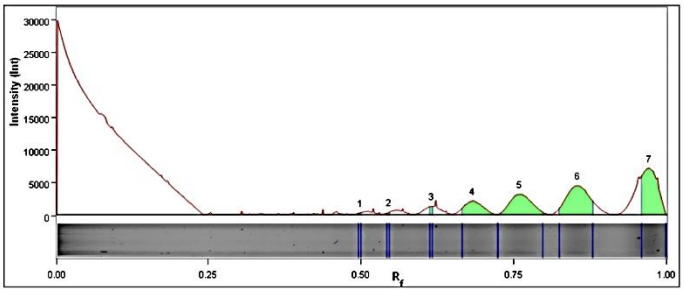

Figure S5: Phosphorylation of PC4 regulates chromatin compaction and consequent histone modification status. Band intensity analysis plot for each of the lanes shown in Fig.5A.

S6

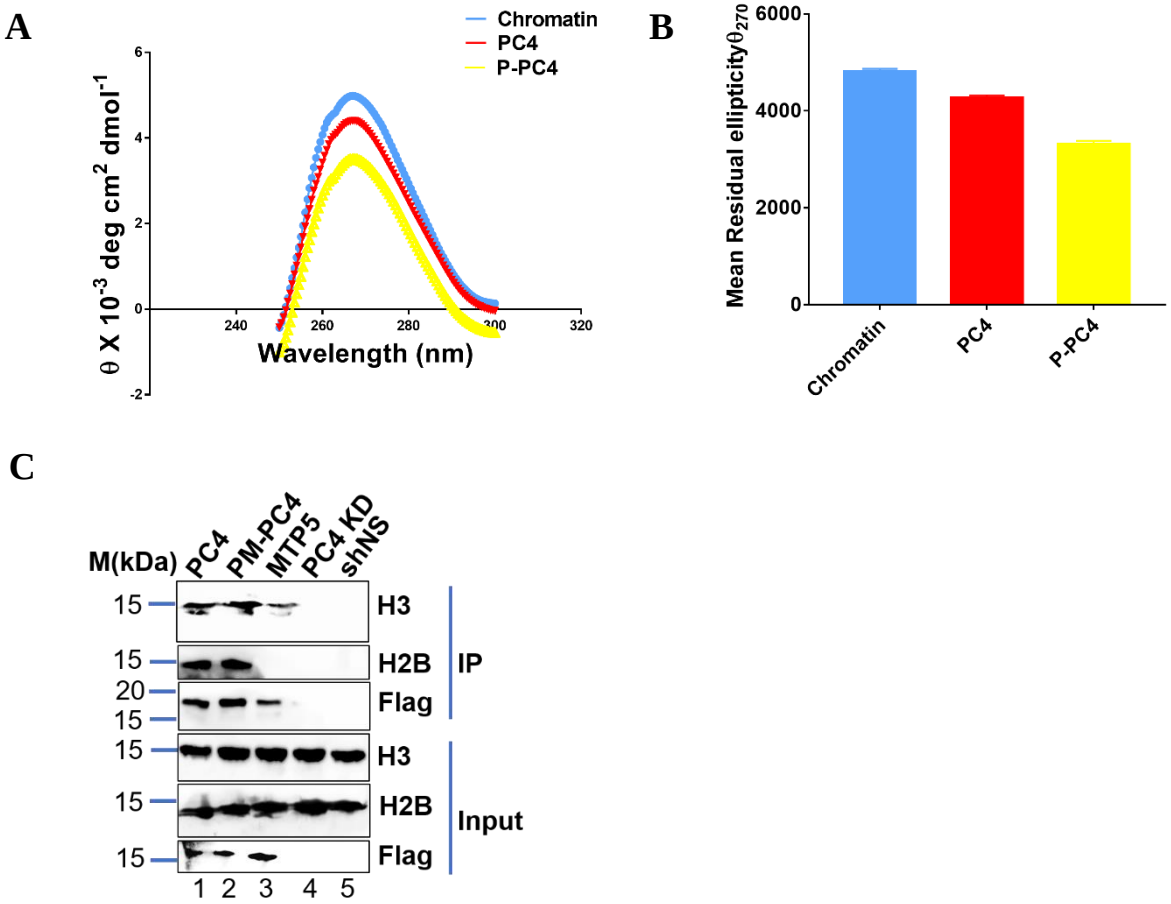

Figure S6: Phosphorylation of PC4 regulates chromatin compaction and consequent histone modification status. (A) Circular dichroism (CD) spectroscopy of P-PC4 and PC4 incubated with H1-stripped chromatin, isolated and purified by sucrose gradient from HeLa cells, for 30 mins and subjected to CD spectroscopy. (B) Quantitative representation of the mean residue ellipticity value plotted for the corresponding CD spectra in (A). (C) Immuno-pulldown using Flag antibody carried out in PC4, PM-PC4 and MTP5 expressing PC4 knockdown cells from the chromatin fraction and probed with H3 and H2B antibody.

S7

A

PC4 vs PC4 KD

Name	Change	Fold change (log2)
TET1	Decreased	-3.02737123
GCM2	Decreased	-2.577207953
RNA5SP38	Decreased	-2.268758224
RP11-65D24.2	Decreased	-2.510963904
LMO7	Decreased	-2.013727828
ZNHIT6	Decreased	-1.79588962
IPMK	Decreased	-1.676840241
FAM204CP	Decreased	-1.545611061
SNRPGP9	Decreased	-1.539182157
PTPRO	Increased	2.035370475
JAKMIP2	Increased	2.334621637
DMRT2	Increased	3.151895985
SYNE1	Increased	3.135653669
ZNF473	Increased	4.005089389
GH1	Increased	4.098320991

B

PM-PC4 vs PC4 KD

Name	Change	Fold change (log2)
RP11-65D24.2	Decreased	-4.092834419
Y_RNA	Decreased	-3.042971151
TET1	Decreased	-2.784275777
RP11-6J24.3	Decreased	-2.608488694
RP11-170N11.1	Decreased	-2.556447887
AC074121.4	Decreased	-2.158780756
FAM204CP	Decreased	-2.132614626
SNRPGP9	Decreased	-2.032164847
DPPA2	Decreased	-1.839925836
MET	Decreased	-1.764417564
JAKMIP2	Increased	2.38
RP11-460N16.1	Increased	2.48
GH1	Increased	3.43
DMRT2	Increased	3.86
RP11-782E2.2	Increased	5.04

C

MTP5 vs PC4 KD

Name	Change	Fold change (log2)
LINC00319	Decreased	-2.4339614
RP11-6J24.3	Decreased	-2.2217879
ADPRHL1	Decreased	-2.1593019
Y_RNA	Decreased	-1.9669342
RP11-170N11.1	Decreased	-1.8461394
SNRPGP9	Decreased	-1.6352571
MIR585	Increased	1.8
MDGA2	Increased	1.81
ATOH8	Increased	2.14
JAKMIP2	Increased	2.28
FGF13-AS1	Increased	2.33
MON2	Increased	2.38
ANKAR	Increased	2.66
DMRT2	Increased	3.31
GH1	Increased	3.88

D

E

F

Overlap of total ATAC-seq peaks with ChIP-seq peaks of different histone marks

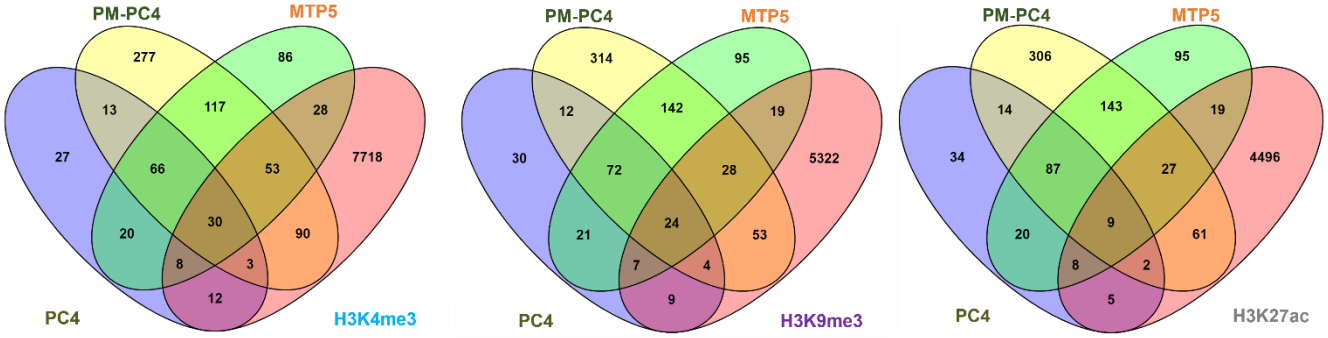

G

H

I

Overlap of Depleted ATAC-seq peaks with ChIP-seq peaks of different histone marks

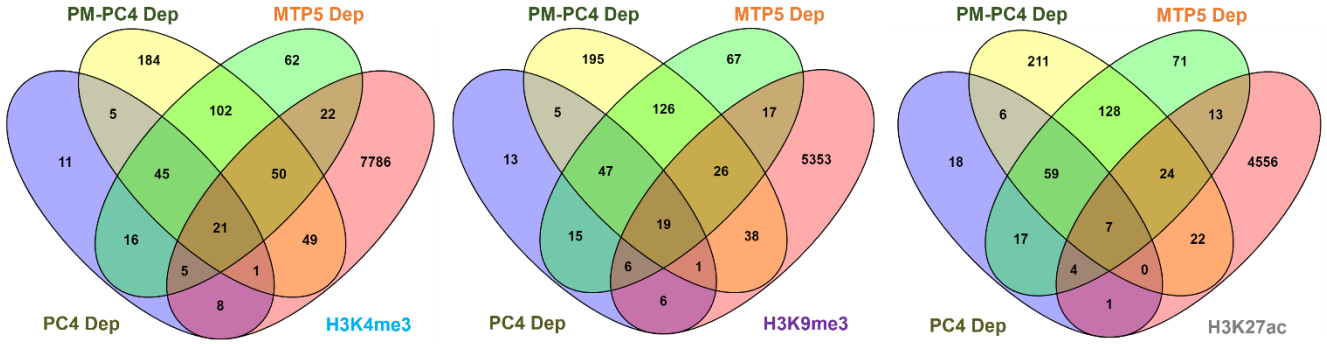

Figures S7: Phosphorylation of PC4 affects chromatin accessibility of various genomic regions harbouring diverse histone marks. (A) List of the top 15 significantly altered ATAC-seq peaks in PC4 relative to PC4 KD. (B) List of the top 15 significantly altered ATAC-seq peaks in PM-PC4 relative to PC4 KD. (C) List of the top 15 significantly altered ATAC-seq peaks in MTP5 relative to PC4 KD. (D) Venn diagram showing the overlap of all the differential ATAC-seq peaks in PC4, PM-PC4 and MTP5 relative to PC4 KD with H3K4me3 ChIP-seq. (E)Venn diagram showing the overlap of all the differential ATAC-seq peaks in PC4, PM-PC4 and MTP5 relative to PC4 KD with H3K9me3 ChIP-seq. (F) Venn diagram showing the overlap of all the differential ATAC-seq peaks in PC4, PM-PC4 and MTP5 relative to PC4 KD with H3K27ac ChIP-seq. (G) Venn diagram showing the overlap of the ATAC-seq peaks depleted in PC4, PM-PC4 and MTP5 relative to PC4 KD with H3K4me3 ChIP-seq. (H) Venn diagram showing the overlap of the ATAC-seq peaks depleted in PC4, PM-PC4 and MTP5 relative to PC4 KD with H3K9me3 ChIP-seq. (I) Venn diagram showing the overlap of the ATAC-seq peaks depleted in PC4, PM-PC4 and MTP5 relative to PC4 KD with H3K27ac ChIP-seq.

S8

A

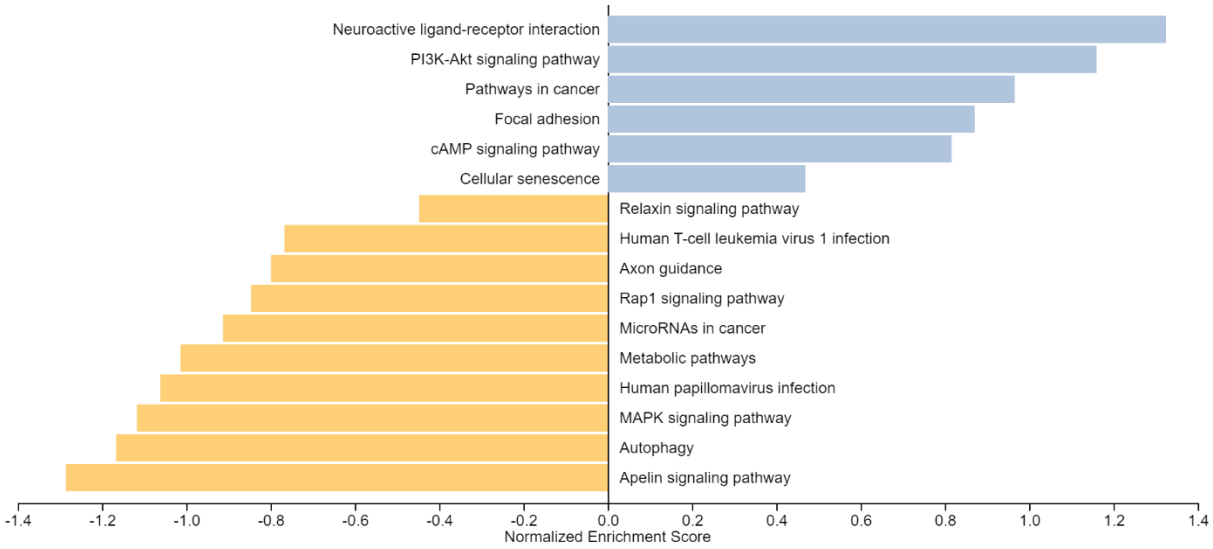
Neuroactive ligand-receptor interaction
PI3K-Akt signaling pathway
Pathways in cancer
Focal adhesion
cAMP signaling pathway
Cellular senescence
Relaxin signaling pathway
Human T-cell leukemia virus 1 infection
Axon guidance
Rap1 signaling pathway
MicroRNAs in cancer
Metabolic pathways
Human papillomavirus infection
MAPK signaling pathway
Autophagy
Apelin signaling pathway
-1.4 -1.2 -1.0 -0.8 -0.6 -0.4 -0.2 0.0 0.2 0.4 0.6 0.8 1.0 1.2 1.4
Normalized Enrichment Score

B

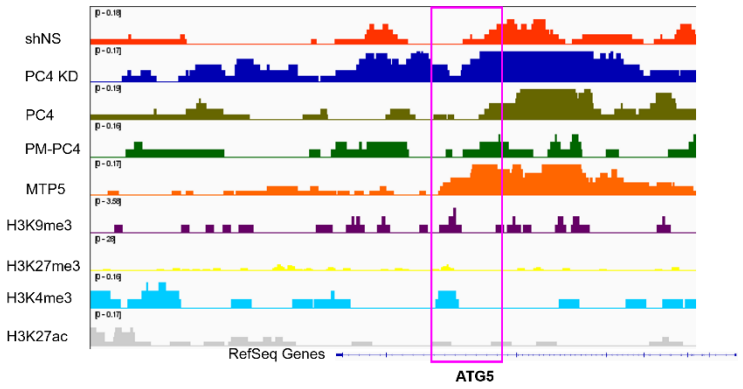
shNS
PC4 KD
PC4
PM-PC4
MTP5
H3K9me3
H3K27me3
H3K4me3
H3K27ac
RefSeq Genes
ATG5

C

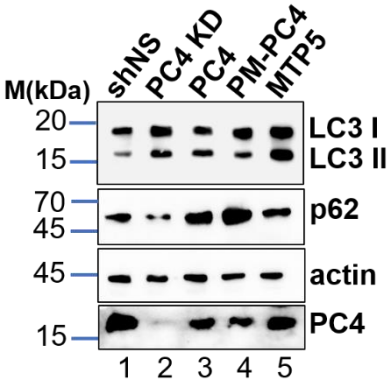
M(kDa)
shNS
PC4 KD
PC4
PM-PC4
MTP5
20
15
LC3 I
LC3 II
70
45
p62
45
actin
15
PC4
1 2 3 4 5

D

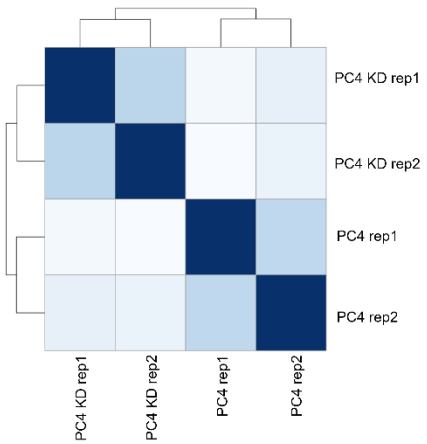
PC4 KD rep1
PC4 KD rep2
PC4 rep1
PC4 rep2
PC4 KD rep1
PC4 KD rep2
PC4 rep1
PC4 rep2

E

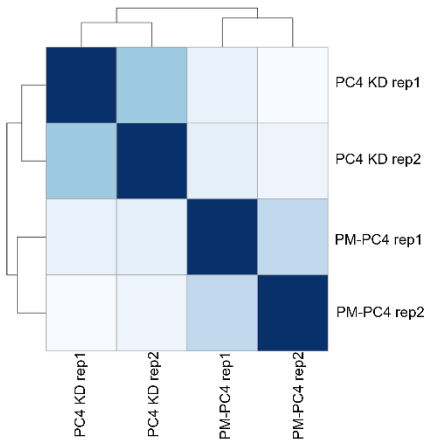
PC4 KD rep1
PC4 KD rep2
PM-PC4 rep1
PM-PC4 rep2
PC4 KD rep1
PC4 KD rep2
PM-PC4 rep1
PM-PC4 rep2

F

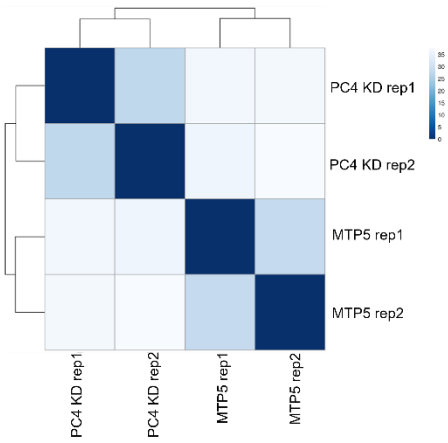
PC4 KD rep1
PC4 KD rep2
MTP5 rep1
MTP5 rep2
PC4 KD rep1
PC4 KD rep2
MTP5 rep1
MTP5 rep2

FigureS8: Phosphorylation of PC4 affects gene transcription by inhibiting chromatin accessibility. (A) GSEA-defined KEGG pathways obtained from mapping the differential ATAC-seq peaks of log2(Fold change) > 1.5 and < -1.5, present in PC4 and PM-PC4 but not present in MTP5 using WEB-based GEne SeT AnaLysis Tool kit (WebGestalt). Positive and negative enrichment scores, respectively, indicate up- and down-regulation of these pathways with respect to PC4 KD cells. (B) Integrative Genomics Viewer (IGV) images showing ATAC-seq intensities in shNS, PC4 KD, PC4, PM-PC4 and MTP5 cells, on representative loci of the core autophagy gene ATG5, along with the published histone modification ChIP seq tracts in HEK293 cells (1–3). (C) Studying the levels of autophagy upon transfecting Flag-PC4 (PC4), Flag-Phosphomimic PC4 (PM-PC4) and Flag-phospho-defective mutant PC4 (MTP5) in PC4 knockdown HEK293 by probing with LC3 and p62 antibody while actin was used as loading control. (D-F) ATAC-seq signal within consensus ATAC-seq peaks was compared between the replicate batches using Spearman's ρ to cluster samples for each of the comparisons; PC4 vs PC4 KD, PM-PC4 vs PC4 KD and MTP5 vs PC4 KD respectively.

Sl. No.	Gene Name	Forward Primer (5'-3')	Reverse Primer (5'-3')
1	*β-Actin*	AGATGTGGATCAGCAAGCAGGAGT	TCCTCGGCCACATTGTGAACTTTG
2	*SCN2*	GCTTTCTGATGTCATGATCTTGACTGTG	CGTGTAGCCATAGTTGGGGTTTCTACC
3	*GAD1*	GCGCCCCACAACGTACGATACC	CACCACTTCCAGGAGGAATTGC
4	*M4*	GGCCTCATGATTGCTGCTGCC	GGCTCTTGAGGAAGGCCAG
5	*AMPKalpha1*	GTCAAAGCCGACCCAATGATA	CGTACACGCAAATAATAGGGGTT
6	*AMPKalpha2*	CAGGCCATAAAGTGGCAGTTA	AAAAGTCTGTCGGAGTGCTGA
7	*ULK1*	GTCACACGCCACATAACAGA	CCATCAAGGTGATGAGGAAGAA
8	*ULK2*	CCCTCCCAAGTCTCATGTTTAG	TCTGATGTGGTTTCCTCTGATG
9	*DRAM1*	GTCAGCCGCCTTCATTATCT	CACTCTCTGGAGGTGTTGTTC
10	*PC4*	AGGTGAGACTTCGAGAGCCCTGT	TTCAGCTGGCTCCATTGTTCTGG
11	*UVRAG*	AGGATTACTTTGTATGCGGTGTC	CAGGTTGGGAAGGGTTTGC
12	*IPMK*	ACCAGCATTACGGAAGAAGCTT	TGGCAGCAACAGCATCTTTT
13	*MAP3K7*	CCGGTGAGATGATCGAAGCC	GCCGAAGCTCTACAATAAACGC
14	*YEATS2*	GGCAGTTGGATACCAGACAGC	CCGCTCACTGGTCCTCATTC

Table S1: Sequences for different real time-PCR primers used for the genes mentioned

Sl. No.	Gene Name	Forward Primer (5'-3')	Reverse Primer (5'-3')
1	*IPMK*	CACCCTGTGCCAAACACATC	AAGCAAGGAGACCCATAAGCC
2	*UVRAG*	GAGATGCTACACCACTCTGCCT	GGATTTACGTTCAGCTACAAGCC
3	*MAP3K7*	GAAGGGTGCATACCAGAC AGA	CTCTGAGCTAGCTGCGTAAGAAT A
4	*HNF4A*	TCCGTTGGCTCTGGATAATG	CACGTAGTGTCCGATCTTCAC

Table S2: Sequences for different ChIP-PCR primers used for the genes mentioned

Analysis of ATAC-seq data

Adapter sequences were trimmed from the raw ATAC-seq reads with CutAdapt v1.121 (4). Trimmed reads of each sample were mapped to the reference human genome build GRCh37/hg19 by using Bowtie2 v2.3.2 with default settings (5). Picard tools (http://broadinstitute.github.io/picard/) v1.126 was used to remove PCR duplicated reads and for insert size distribution analysis. Reads mapping to mitochondrial DNA and the Y chromosome were filtered and only uniquely mapping paired reads with a quality score≥30 were kept for subsequent analysis. The read start sites were adjusted to represent the center of the transposon binding event (5bp on forward strand and 4bp on reverse strand) as described (6). Phantompeakqualtools v2.0 was used to calculate the strand cross-correlation and deepTools v2.0.1 was used to calculate correlation between samples (7). MACS2 v2.1.0 was used for peak calling with parameters "--nomodel--nolambda-keep-dup all--call-summits-g hs-B", and peaks were filtered based on default settings and false discovery rate (FDR) < 0.1 (8). Peaks in regions known to show artificially high signal were filtered using the hg19 blacklist file from ENCODE. BEDTools v2.26.07 was used for various analyses based on peak locations. Peaks located less than 50bp apart were merged in order to facilitate comparison between samples. The whole ATAC-seq workflow was implemented in Snakemake. All sequencing track figures were generated with the integrative genome browser (IGV).

Gene Set Enrichment Analysis (GSEA):

GSEA method was carried out using pathway- KEGG enrichment category using WebGestalt (WEB-based Gene SeT AnaLysis Toolkit) functional enrichment analysis web tool (9–11).

Antibodies

Anti-PC4 (in-house-generated polyclonal antibody), anti-histone H3 (in-house-generated polyclonal antibody), anti-histone H2B (in-house-generated polyclonal antibody), anti-H3K9ac (Abcam, ab16635, Cambridge,UK), anti-H3K4me3 (Millipore, #07-473), anti-H2B tetra-acetylation (Millipore, #07-373), anti-H3K9me2 (abcam, 1220), anti-FLAG (Sigma, F1804, Lot no. SLBK1346V), anti-actin HRP conjugated (Sigma), Goat Anti-Rabbit IgG H&L (HRP; Abcam, Cat No. ab97051, Lot No. GR288027-9), Goat Anti-Mouse IgG H&L (HRP; Abcam, Cat No. ab97023, Lot No. GR298142-12), F(ab')2-Goat anti-mouse IgG (H + L) Cross-Adsorbed Secondary Antibody, Alexa Fluor 568 (A11004, RRID:AB_2534072, Life Technologies), anti-H1.2 (abcam, Cat No. ab181973), anti-H1 (in-house-generated polyclonal antibody), anti-p62 (Sigma P0067), anti-MAP1LC3B (Sigma L7543).

References:

1. Hattori,T., Lai,D., Dementieva,I.S., Montaño,S.P., Kurosawa,K., Zheng,Y., Akin,L.R., Świst-Rosowska,K.M., Grzybowski,A.T., Koide,A., *et al.* (2016) Antigen clasping by two antigen-binding sites of an exceptionally specific antibody for histone methylation. *Proceedings of the National Academy of Sciences of the United States of America*, **113**, 2092–7.

2. Lamb,K.N., Bsteh,D., Dishman,S.N., Moussa,H.F., Fan,H., Stuckey,J.I., Norris,J.L., Cholensky,S.H., Li,D., Wang,J., *et al.* (2019) Discovery and Characterization of a Cellular Potent Positive Allosteric Modulator of the Polycomb Repressive Complex 1 Chromodomain, CBX7. *Cell chemical biology*, **26**, 1365-1379.e22.

3. Morgan,M.A.J., Rickels,R.A., Collings,C.K., He,X., Cao,K., Herz,H.-M., Cozzolino,K.A., Abshiru,N.A., Marshall,S.A., Rendleman,E.J., *et al.* (2017) A cryptic Tudor domain links BRWD2/PHIP to COMPASS-mediated histone H3K4 methylation. *Genes & development*, **31**, 2003–2014.

4. M,M. (2011) Cutadapt Removes Adapter Sequences From High-Throughput Sequencing Reads. *EMBnet.journal*, **17**, 10-12.

5. Langmead,B. and Salzberg,S.L. (2012) Fast gapped-read alignment with Bowtie 2 : Nature Methods : Nature Publishing Group. *Nat Meth*, **4**, 357-9.

6. Buenrostro,J.D., Giresi,P.G., Zaba,L.C., Chang,H.Y. and Greenleaf,W.J. (2013) Transposition of native chromatin for fast and sensitive epigenomic profiling of open chromatin, DNA-binding proteins and nucleosome position. *Nature Methods*, **10**, 1213-8.

7. Ramírez,F., Ryan,D.P., Grüning,B., Bhardwaj,V., Kilpert,F., Richter,A.S., Heyne,S., Dündar,F. and Manke,T. (2016) deepTools2: a next generation web server for deep-sequencing data analysis. *Nucleic acids research*, **44**, W160-5.

8. Zhang,Y., Liu,T., Meyer,C.A., Eeckhoute,J., Johnson,D.S., Bernstein,B.E., Nussbaum,C., Myers,R.M., Brown,M., Li,W., *et al.* (2008) Model-based analysis of ChIP-Seq (MACS). *Genome Biology*, **9**, R137.

9. Zhang,B., Kirov,S. and Snoddy,J. (2005) WebGestalt: An integrated system for exploring gene sets in various biological contexts. *Nucleic Acids Research*, **33**, W741-8.

10. Wang,J., Vasaikar,S., Shi,Z., Greer,M. and Zhang,B. (2017) WebGestalt 2017: A more comprehensive, powerful, flexible and interactive gene set enrichment analysis toolkit. *Nucleic Acids Research*, **45**, W130-W137.

11. Liao,Y., Wang,J., Jaehnig,E.J., Shi,Z. and Zhang,B. (2019) WebGestalt 2019: gene set analysis toolkit with revamped UIs and APIs. *Nucleic Acids Research*, **47**, W199-W205.